Journal of Systems Engineering and Electronics
Vol. 33, No. 5, October 2022, pp.1025 – 1031

Half space object classification via incident angle based fusion of radar and infrared sensors

HE Zhenyu[1,2], ZHUGE Xiaodong[1], WANG Junxiang[3], YU Shihao[1],
XIE Yongjun[1,4,*], and ZHAO Yuxiong[5]

1. School of Electronic Information and Engineering, Beihang University, Beijing 100191, China;
2. Beijing Institute of Electronic System Engineering, Beijing 100854, China;
3. Beijing Institute of Astronautical Systems Engineering, Beijing 100076, China;
4. Shenzhen Institute of Beihang University, Shenzhen 518038, China;
5. School of Software, Beihang University, Beijing 100191, China

Abstract: In this paper, we introduce an incident angle based fusion method for radar and infrared sensors to improve the recognition rate of complex targets under half space scenarios, e.g., vehicles on the ground in this paper. For radar sensors, convolutional operation is introduced into the autoencoder, a "winner-take-all (WTA)" convolutional autoencoder (CAE) is used to improve the recognition rate of the radar high resolution range profile (HRRP). Moreover, different from the free space, the HRRP in half space is more complex. In order to get closer to the real situation, the half space HRRP is simulated as the dataset. The recognition rate has a growth more than 7% compared with the traditional CAE or denoised sparse autoencoder (DSAE). For infrared sensor, a convolutional neural network (CNN) is used for infrared image recognition. Finally, we combine the two results with the Dempster-Shafer (D-S) evidence theory, and the discounting operation is introduced in the fusion to improve the recognition rate. The recognition rate after fusion has a growth more than 7% compared with a single sensor. After the discounting operation, the accuracy rate has been improved by 1.5%, which validates the effectiveness of the proposed method.

Keywords: convolutional autoencoder (CAE), half space, high-resolution range profile (HRRP), incident angle based fusion, target recognition.

DOI: 10.23919/JSEE.2022.000100

1. Introduction

In view of the increasing complexity of modern battlefield environment, the current missile-borne platforms mostly use a radar/infrared composite form for fusion-based target recognition. The main challenges for fusion-based recognition from multisensory data include experimental data acquisition, feature extraction, classification and data fusion methods.

The radar sensor has the ability to work all-weather under complex climate conditions, and is not easily interfered by weather factors such as fog. It is a very common tool in modern battlefield. High resolution range profile (HRRP) of the target can be obtained by radar sensor. HRRP is the vector sum of the complex echoes from scatterer centers of a target from the radar line-of-sight (LOS) [1]. An HRRP contains the structural information of the target and can be easily obtained and processed. Thus, the radar automatic target recognition (RATR) classification method based on HRRPs has been widely developed. However, an HRRP is extremely vulnerable to clutters in practice, especially in half-space environment. Half space can be divided into upper half space and lower half space. The media of the two spaces are different. The vehicle on the ground can be regarded as a half space target, which is at the junction of two different media: air and ground. The ground clutter distributes widely, which results in huge differences between half space HRRPs and free space HRRPs, making accurate target recognition more difficult.

In order to solve this problem, this paper uses a high frequency algorithm to simulate the HRRPs of objects in half space [2]. The high frequency algorithm is to introduce the half-space Green's function into the conventional physical optics method, using a graphical-electromagnetic computing method, the radar cross-section of conductive targets can be calculated in half-space. The graphical-electromagnetic computing method [3] adds an appropriate lighting mode to the physical models, deter-

Manuscript received August 13, 2020.
*Corresponding author.
This work was supported by the National Natural Science Foundation of China (61571022; 61971022).

mines the three primary colors intensity components of each element, and then calculates the value. Recently, using deep learning, RATR based on HRRPs has been widely studied [4−7]. In [4], a denoising sparse autoencoder was proposed on airplane target recognition and obtained a good performance. Stacked autoencoder and extreme learning machine were used for target recognition in [7]. However, most of the targets are that in free space. Therefore, these methods are more suitable for feature extraction and classification of free space HRRP. Compared with free space, the structure of HRRP in half space is more complex. Compared with the traditional architecture, convolution architecture has a better performance on coding and feature extraction. In this paper, a stacked convolutional autoencoder (SCAE) [8] is used to extract the features of half space HRRP samples.

An HRRP is susceptible to electromagnetic interference, while infrared images are not affected by ground clutter or sea clutter, that is, they are immune to half space environment and insensitive to azimuth. Therefore, the shortage of radar sensors can be compensated by collecting and classifying infrared images. A convolutional neural network is used to extract the high abstract features of the infrared images and a softmax classifier is used to classify the targets.

Although the infrared sensor can make up for the shortage of radar sensor, the infrared sensor itself is easy to be affected by the weather and has a short detection distance. Due to the respective disadvantages of radar sensors and infrared sensors, the reliability of classification results obtained by a single sensor is not stable. Therefore, combining the two results to detect a target is a feasible method, which should effectively improve the recognition rate. Multisensory information fusion can be categorized into data-level fusion, feature-level fusion and decision-level fusion. Comparing with the first two, decision-level fusion requires less information and processing. The Dempster-Shafer (D-S) theory is flexible and is widely used in recent years [9−11]. In this paper, the decision fusion method based on the D-S evidence theory is used to fuse the recognition results of the radar and infrared sensors. We also analyze the relationship between the pitching angle and the discount coefficient and use discounting operation to reduce the dependence of recognition results on sensors with low credibility.

The rest of the article is organized as follows. Section 2 introduces the feature extraction methods and the steps of decision fusion in detail. Recognition results of half space targets at different incident angles before and after fusion are compared to examine the validity of the method in Section 3. Section 4 summarizes the results and conclusions of this paper.

2. Methods

2.1 HRRP characteristics of half space targets

For targets in free space, the propagation path of the wave is single and the echoes received by radar mainly come from the targets. However, in practical applications, the ground, i.e., half space is located on radar LOS. Waves will scatter between the ground and the target, which makes the echoes received by the radar more complex. As shown in Fig. 1(b), different from the free space, the waves will scatter many times between the target and the ground in half space environment. This makes the echoes received by the radar different, and makes the HRRPs different. The path of echoes in free space is only path A, but echoes in half space travel along path A, path B and path C. Fig. 1(a) shows the HRRPs of T-80 Main Battle Tank in half space and free space. Building a model for targets in half space based on targets in free space cannot work well since their HRRP samples are too different, as demonstrated in Fig. 1(a). Therefore, it is obvious that half space HRRP samples perform far better than the free space HRRP samples when training the model.

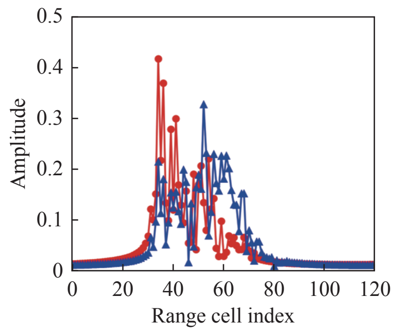

(a) HRRPs of T-80

: Free space; : Half space.

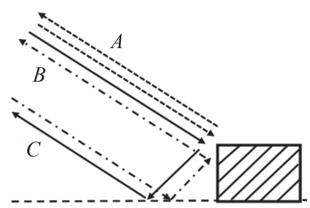

(b) Echoes

Fig. 1 HRRP and echoes in half space and free space

2.2 Feature extraction of radar HRRP based on SCAE

First, L2 normalization is used to remove the amplitude sensitivity of the HRRPs. Then, an SCAE is used to extract features from the normalized HRRPs. Finally, an LSVM is used to classify the targets by using the extracted features as the input.

Autoencoder is an unsupervised learning algorithm, which consists of an encoder and a decoder. Autoencoder can extract the important information of the input by making the output as similar to the input as possible. The encoder uses the input x to calculate the hidden representation, and the decoder uses the hidden representation h to reconstruct the input x. $\hat{x}$ is the output of the decoder.

$$\boldsymbol{h} = \sigma(\boldsymbol{W}\boldsymbol{x} + \boldsymbol{b}), \tag{1}$$

$$\hat{\boldsymbol{x}} = \sigma(\boldsymbol{W}'\boldsymbol{h} + \boldsymbol{b}'), \tag{2}$$

where $\boldsymbol{W}$ and $\boldsymbol{W}'$ are the weight matrices, and $\boldsymbol{b}$ and $\boldsymbol{b}'$ are the bias vectors. We make $\hat{\boldsymbol{x}}$ close to $\boldsymbol{x}$ by training $\boldsymbol{\theta} = (\boldsymbol{W}, \boldsymbol{b})$, whose loss function is

$$L = \sum_{i=1}^{n} \|\hat{\boldsymbol{x}}_i - \boldsymbol{x}_i\|^2 . \tag{3}$$

A stack autoencoder (SAE) is the stack of multiple autoencoders. An SAE extracts features layer by layer, and can get deeper and more abstract features. A convolution computation [12] is introduced into the encoding and decoding layers to explicitly take spatial information into account. $\boldsymbol{W}x$ is replaced by $\boldsymbol{W}*\boldsymbol{x}$ and $\boldsymbol{W}'\boldsymbol{h}$ is replaced by $\boldsymbol{W}'*\boldsymbol{h}$. $(\cdot)*$ means convolution multiplication.

In order to enhance the performance of the convolutional autoencoder (CAE), we add a constraint called winner-take-all (WTA) sparsity [13]. The constraint is composed of spatial sparsity and life sparsity. When using spatial sparsity constraints, in the training phase, the output is not directly reconstructed from the hidden layer data, but from the largest unit in the feature map of the hidden layer, while the other units are zeroed. In the testing phase, the condition is closed and an additional ReLU layer is used to process the feature map, and then a maximum pooling is applied to get the output. Life sparsity is a further constraint based on spatial sparsity. In training, only the first $k\%$ non-zero hidden units are retained in the mini-batch samples, and the rest are set to zero. These restrictions can force the model to extract the robust features of the HRRPs. A WTA-CAE is shown in Fig. 2. The input is the simulated HRRP, and the output is the reduced HRRP after decoding.

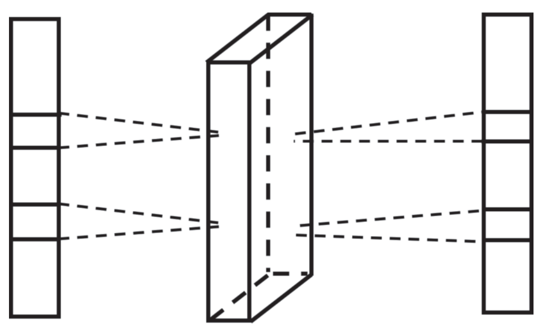

Fig. 2 WTA-CAE

2.3 Infrared image recognition based on convolutional neural network (CNN)

The infrared image is related to the temperature of the target. When the temperature of the target is higher than absolute zero, infrared radiation will be generated, and the radiation intensity can be distinguished by color. The higher the temperature of the same object, the greater the amount of radiation generated, and the greater the brightness of its infrared image. For example, the temperature of the engine will rise when the vehicle is driving, and the tire will have higher temperature due to friction with the ground, so the brightness of the corresponding part of its infrared image is high.

In recent years, the CNN has developed rapidly and it can extract the features of the image effectively. Some researchers have used CNN to process infrared images, and achieved good results [14,15]. After normalizing the infrared images, a CNN is used for feature extraction, and a softmax classifier is used for classification.

Fig. 3 shows the structure of the CNN which we used in infrared images' recognition.

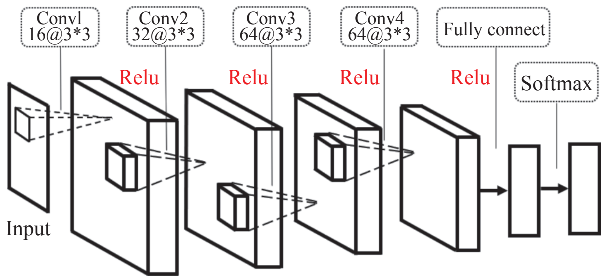

Fig. 3 Structure of CNN

2.4 Decision fusion based on D-S theory

The fusion follows the classification. Before fusion, we need to calculate the basic probability assignment (BPA) of each sensor's classification result. Then, we use the D-S theory to combine the BPA of each sensor, and get the final classification result. The BPA is the degree of trust assigned to each proposition in the hypothesis space. BPA cannot satisfy the countable additivity and it is the evaluation weight of various hypotheses, but not the probability. $\text{BPA} \in [0, 1]$ and the sum of BPA of each proposition in hypothesis space is 1. Thus, first, the BPA of each proposition in the hypothesis space is calculated before fusion.

For radar HRRP target recognition, the HRRP obtained by radar sensor is a 1×128 vector, the data is relatively simple, and there are only three categories of classification tasks, so the support vector machine (SVM) is used for classification. In the three classification tasks, an SVM consists of three linear SVMs (LSVM). For every sample x, each LSVM classifier will output a scoring function $f_i(x)$, and we can get

$$y_i = \text{sign}(f_i(x)). \tag{4}$$

If $y_i = 1$, the classifier considers that the sample belongs to category i, and a larger $f_i(x)$ indicates stronger credibility. However, it does not mean that the sample is 100% classified as category i. Only a probability of $1-\exp(-|f_i(x)|)$ determines that it is category i. Since a classification threshold is used, a small percentage of targets is still misclassified, which is represented by the hypothesis space H. The whole hypothesis space is a complete space in which elements do not intersect each other, $H = \{h_i, \overline{h_i}\}$, h_i means the target is determined as category i, $\overline{h_i}$ indicates that the target is not classified as category i. Thus, when $y_i = 1$, the BPA formula is as follows:

$$m_1(\pi) = \begin{cases} 1-\exp(-|f_i(x)|), & \pi = \{h_i\} \\ \exp(-|f_i(x)|), & \pi = H \\ 0, & \text{otherwise} \end{cases}. \tag{5}$$

If $y_i = -1$, the sample is considered not to belong to category i. Therefore, the BPA formula is as follows:

$$m_1(\pi) = \begin{cases} 1-\exp(-|f_i(x)|), & \pi = \{\overline{h_i}\} \\ \exp(-|f_i(x)|), & \pi = H \\ 0, & \text{otherwise} \end{cases}. \tag{6}$$

The infrared image obtained by infrared sensor is a 256×256 image, which is more complex. At present, CNN can better classify the images, and the softmax classifier can achieve better results for the classification tasks of different kinds of targets. Thus, a softmax classifier is used to classify infrared images. A softmax classifier is a multi-classifier (three categories in this paper). Its output is a multi-dimensional vector (three dimensions in this paper):

$$\boldsymbol{a} = (a_1, a_2, a_3) \tag{7}$$

where a_i is the probability that the sample belongs to Category i, so its BPA formula is as follows:

$$m_2(\pi) = a_i, \quad \pi = \{h_i\}. \tag{8}$$

The BPA for A after fusion is as follows:

$$m(A) = \frac{1}{N} \sum_{E \cap F = A} m_1(E) m_2(F), \quad A \neq \varnothing, \tag{9}$$

$$N = \sum_{E \cap F \neq \varnothing} m_1(E) m_2(F), \tag{10}$$

where E and F are the BPA based on different sensors. When classifying the same target, different sensors may have different results, and the same sensor may also consider the target to belong to different types. The above formula is to fuse the parts of the result that contain the same category, and get the BPA that the target belongs to each category.

The category corresponding to the maximum value of BPA is the final classification result.

Each sensor has its own shortages. In some cases, the reliability of the radar sensors is lower than that of the infrared sensors, while it sometimes is the opposite. This problem can be alleviated by introducing discounting operation [16]. If the reliability of a sensor is known to be α, which is called discount coefficient, the BPA is as follows:

$$m^{\alpha}(A) = (1-\alpha)m(A), \quad A \in H, \tag{11}$$

$$m^{\alpha}(H) = \alpha + (1-\alpha)m(H). \tag{12}$$

In target recognition, the greater the difference in HRRPs between different targets, the easier it is to identify them. At some pitching angles, the HRRPs of different targets have great similarity, which makes the target recognition difficult. When the pitching angle is too large or too small, because of the high similarity of HRRPs between different targets, the recognition rate based on the radar sensor is low. We believe the credibility of the radar sensor is low. However, when we fuse the results of the two sensors, it is generally assumed that the credibility of the two sensors is the same. This makes the final recognition accuracy not very ideal. Therefore, we need to make a discount on the radar sensor at these angles. The discount coefficient is used to reduce the BPA of the sensor. The larger the discount coefficient is, the smaller the BPA is, and the less dependent the final result is on radar sensor. Thus, we can improve the recognition rate by introducing a discounting operation into the result of HRRP recognition.

The fusion process is shown in Fig. 4.

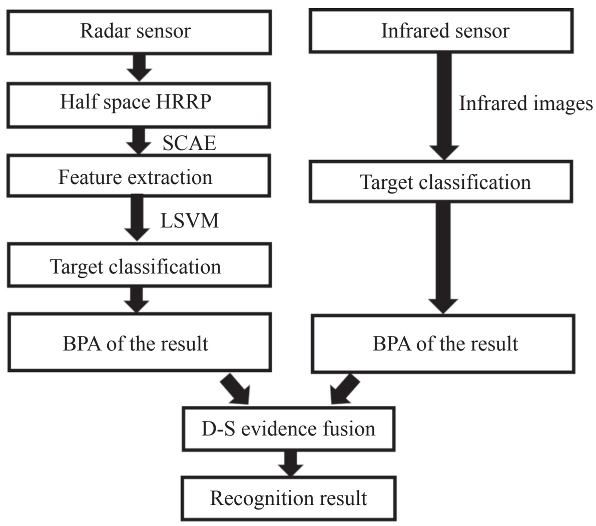

Fig. 4 Process of decision fusion recognition

3. Experiments and discussion

3.1 Data set

This paper verifies the validity of the proposed method using the data of three targets, including T-80 Main Battle Tank, UAZ-469 off-road Vehicle and URAL-4320 Truck. The models corresponding to three targets are shown in Fig. 5. The specific parameters are given in Table 1. Both the HRRPs and infrared images used for the experiments are simulated. The sizes of HRRPs and infrared images are 1×128 and 512×512.

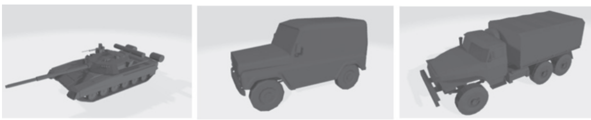

(a) T-80 (b) UAZ-469 (c) URAL-4320

Fig. 5 Models of the three kinds of targets

Table 1 Dimensional parameters of targets m

Target	Length	Width	Height
T-80	9.720	3.560	2.740
UAZ-469	4.025	1.785	2.050
URAL-4320	7.366	2.500	3.005

For HRRP data, in order to make the dataset more complete, we calculate the data of three kinds of targets in half space and free space. The aspect angle and the pitching angle of the targets change gradually. The aspect angle changes from 0° to 90° (with 1° interval), and the pitching angle changes from 10° to 80° (with 1° interval). Thus, there are 90 samples under each pitching angle. The half-space data of odd pitching angles is used for training, while the data of even pitching angles is used for testing. This operation makes the training set cover all cases of half space target as much as possible.

Four experiments are conducted to validate the necessity of the half space dataset (pitching angle of the data changes from 17° to 42°). Without any feature extraction, an LSVM is directly used to classify the targets. The design of the three experiments is as follows: (i) free space data is used as training set and test set; (ii) free space data is used as training set and half space data is used as test set; (iii) half space data is used as training set and test set; (iv) half space data is used as training set and free space data is used as test set. The results are listed in Table 2. These results average over all three target types.

As shown in Table 2, the models trained by different training sets are extremely different, and due to the more complex structure of half space HRRP, the recognition rate of the half space HRRP is much lower than that of free space HRRP.

Table 2 Recognition result by SVM

Training set	Test set	Recognition rate/%
Free space	Free space	82.24
Free space	Half space	39.60
Half space	Half space	75.64
Half space	Free space	69.34

For infrared images, Wang et al. [17] proposed a model for calculating infrared images of ground targets, and we use it to simulate the infrared images of the three targets in this paper. The infrared images of the three kinds of targets are shown in Fig. 6. Three samples of each target at every odd pitching angle are chosen as the training set, while the infrared images of each target at even pitching angle and aspect angle are chosen as the test set.

(a) T-80 (b) UAZ-469 (c) URAL-4320

Fig. 6 Infrared images of the three kinds of targets

3.2 Recognition result of single sensor

In this paper, for radar sensor, we use WTA-SCAE to extract high-dimensional features of HRRP data. The extracted features, as the input, are classified by an LSVM. The proposed WTA-SCAE's structure is as follows. In the first layer of the SCAE, 64 filters with a 15 × 1 receptive field applied at strides of 1 pixel are used. In the classification time, we use max pooling over 6×1 regions at strides of three pixels to obtain the final 64×37 representations. In the second layer, we train another 512 feature maps on top of the pooled feature maps of the first layer, with a 5×1 receptive field at strides of one pixel. In the classification time, we use max pooling over 3×1 regions at strides of two pixels to obtain the final 512×16 representation. And a ReLU is used as the activation function. A denoised SAE (DSAE) is robust to noise, and it can encode and decode the noisy/imperfect data. Thus DSAE has a wide range of applications in target recognition based on HRRP. In order to prove the superiority of WTA-SCAE, we compare the recognition rate based on WTA-SCAE, WTA-CAE, DSAE and traditional CAE. The recognition rates obtained by different methods are listed in Table 3. The data used in the experiment is the half space HRRP.

Table 3 Comparison of DSAE, CAE, WTA-CAE, and WTA-SCAE

%

Target	DSAE	CAE	WTA-CAE	WTA-SCAE
T-80	68.40	69.51	71.57	74.41
UAZ-469	67.40	64.97	74.29	76.14
URAL-4320	68.72	68.49	74.40	75.03
Average	68.17	67.66	73.42	75.29

Compared with DSAE and CAE, the proposed method achieves the best recognition performance. The target recognition rate based on WTA-SCAE is 7.63% higher than that based on CAE and 7.12% higher than that based on DSAE. That is, the performance of WTA-SCAE is better than the other two methods in feature extraction.

As shown in Fig. 7, though, compared with DSAE, CAE and WTA-CAE, the recognition rate based on WTA-SCAE is higher, and the recognition rate based on infrared images is also high, the recognition rate of some pitching angles is still far below the average, and the average recognition rate is not up to 90%. Therefore, the recognition rate needs to be improved.

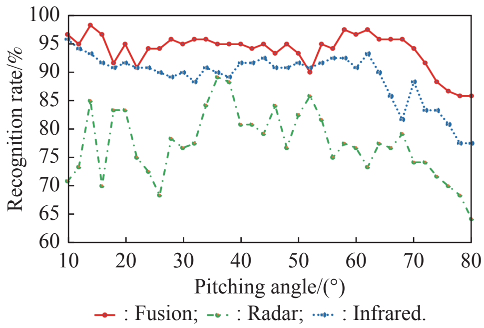

Fig. 7 Recognition rate after fusion

3.3 Recognition result of incident angle based fusion

The recognition results of the two sensors are fused by the decision fusion method based on D-S theory, and the fusion results of all pitching angles are shown in Fig. 7, the recognition rate based on decision fusion is higher than that of a single sensor. The recognition accuracy of the infrared sensor is higher than that of the radar sensor, but it only reaches 89.3%. After fusion, the average recognition accuracy reaches 94.4%, which is more than 5% higher than that of a single sensor. Moreover, the recognition rate is improved by 8.34% compared with a single sensor when the pitching angle is 72°. Therefore, the decision fusion recognition method can be used in target recognition.

However, when the pitching angle is too large or too small, the reliability of the radar sensor is relatively low because of the high similarity of HRRP between different targets in these angles. To improve the recognition rate, discounting operation is used to reduce the dependence of recognition rate on the radar sensor. The discount coefficient is limited from 0 to 1 (the interval is 0.1).

The recognition result with the discounting operation is shown in Fig. 8. When the pitching angle is less than 24° or between 52° and 66°, the HRRP's similarity of different targets is large, and the reliability of the radar sensor is low. At this time, discounting operation (discount coefficient = 0.1) is used to further improve the recognition rate. When the pitching angle is greater than 66°, the HRRP similarity of different targets is larger, so the reliability of the sensor is lower. At this time, discounting operation (discount coefficient is 0.2) is used to further improve the recognition rate. When the pitching angle is between 24° and 50°, because of the high reliability of the radar sensor, discounting operation is not needed (discount coefficient is 0) to obtain a high recognition rate.

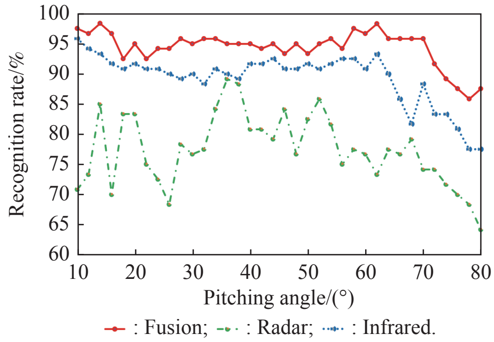

Fig. 8 Recognition rate after discounting operation

The fusion with discounting operation performs better than that without discounting operation. After discounting operation, the recognition rate of most pitching angles is increased by 1.5% on average. Moreover, when the pitching angle is 52°, the recognition rate is increased by 5%.

4. Conclusions

In this paper, we introduce an incident angle based fusion method of radar/infrared sensor for target recognition, which can improve classification performance. The WTA-SCAE approach outperforms CAE and DSAE, and the features extracted by the WTA-SCAE are more robust compared with the other two methods. Data fusion can reduce the instability of a single sensor due to environmental influences. And with a certain fault tolerance capability, the decision-level fusion is a high-level fusion, which can get the correct results when a sensor has errors. The recognition rate after fusion is much higher than that of a single sensor. Moreover, the discounting operation has a better performance in overcoming the dependence of the unreliable sensor. The experimental results validate the effectiveness of the method.

References

[1] GAO F, HUANG T, WANG J, et al. A novel multi-input bidirectional LSTM and HMM based approach for target

recognition from multi-domain radar range profiles. Electronics, 2019, 8: 535.
[2] LI X F, XIE Y J, WANG P, et al. High-frequency method for scattering from electrically large conductive targets in half-space. IEEE Antennas and Wireless Propagation Letters, 2007, 6: 259–262.
[3] RIUS J M, FERRANDO M. GRECO: graphical electromagnetic computing for RCS prediction in real time. IEEE Antennas & Propagation Magazine, 1993, 35(2): 7–17.
[4] YAN H Q, ZHANG Z H, XIONG G, et al. Radar HRRP recognition based on sparse denoising autoencoder and multi-layer perceptron deep model. Proc of the Fourth International Conference on Ubiquitous Positioning, Indoor Navigation and Location Based Services, 2016: 283–288.
[5] ZHANG Y X, WANG X D, YAO X, et al. HRRP recognition for polarization radar based on Bagging-SVM dynamic ensemble. Systems Engineering and Electronics, 2012, 34(7): 1366–1371. (in Chinese)
[6] YUAN J, LIU W, ZHANG G. Application of dictionary learning algorithm in HRRP based on statistical modeling. Systems Engineering and Electronics, 2018, 40(4): 762–767. (in Chinese)
[7] TAI G X, WANG Y H, LI Y, et al. Radar HRRP target recognition based on stacked denosing sparse autoencoder. The Journal of Engineering, 2019, 2019(21): 7945–7949.
[8] YU S H, XIE Y J. Application of a convolutional autoencoder to half space radar HRRP recognition. Proc of the International Conference on Wavelet Analysis and Pattern Recognition, 2018: 48–53.
[9] JIAO Z B, WANG Y F. A D-S evidence theory-based relay protection system hidden failures detection method in smart grid. Proc. of the IEEE Power & Energy Society General Meeting, 2017. DOI: 10.1109/PESGM.2017.8274673.
[10] SHEN X H, LIU K Y, LIU Z, et al. A wind turbine fault diagnosis method using adaptive weighting algorithm and D-S evidence theory. Proc. of the IEEE 2nd Advanced Information Management, Communicates, Electronic and Automation Control Conference, 2018: 626–630.
[11] DONG G G, KUANG G Y. Target recognition via information aggregation through Dempster–Shafer's evidence theory. IEEE Geoscience and Remote Sensing Letters, 2015, 12(6): 1247–1251.
[12] MASCI J, MEIER U, CIRESAN D, et al. Stacked convolutional auto-encoders for hierarchical feature extraction. Artificial Neural Networks and Machine Learning, 2011: 52–59.
[13] MAKHZANI A, FREY B J. Winner-take-all autoencoders. Proc. of the 28th International Conference on Neural Information Processing Systems, 2015, 2: 2791–2799.
[14] GU J X, WANG Z H, KUEN J, et al. Recent advances in convolutional neural networks. Pattern Recognition, 2018, 77(C): 354–377.
[15] MOATE C P, HAYWARD S D, ELLIS J S, et al. Vehicle detection in infrared imagery using neural networks with synthetic training data. Proc. of the International Conference Image Analysis and Recognition, 2018: 453–461.
[16] MERCIER D, QUOST B, DENŒUX T. Refined modeling of sensor reliability in the belief function framework using contextual discounting. Information Fusion, 2008, 9(2): 246–258.
[17] WANG Z Y, WU Z H, BAO H J, et al. Synthesis of infrared ground target and its background. https://doi.org/10.1117/12.441571.

Biographies

HE Zhenyu was born in 1994. He received his B.S. degree from the School of Electronic Information and Engineering from Beihang University, Beijing, China. He is currently studying in Beihang University for his M.S. degree. His current interests include radar target recognition in half space and artificial intelligence.
E-mail: hzy1015@buaa.edu.cn

ZHUGE Xiaodong was born in 1982. He received his M.S. and Ph.D. degrees from the Faculty of Electrical Engineering, Mathematics and Computer Science, Delft University of Technology, the Netherlands, in 2006 and 2010, respectively. From 2011 to 2014, he was a Research Scientist at FEI Electron Optics, Eindhoven, the Netherlands. He was with the National Research Institute for Mathematics and Computer Science, the Netherlands as a Researcher from 2014 to 2017. Since 2017, he has been an associate professor with Beihang University, Beijing, China. His research interests include microwave and millimeter wave sensing and systems, with a strong focus on near-field imaging and measurements.
E-mail: zhuge@buaa.edu.cn

WANG Junxiang was born in 1987. He received his M.S. degree in School of Automation at Northwestern Polytechnical University. He is now working at Beijing Institute of Astronautical Systems Engineering. His research interests are controlled modeling and radar.
E-mail: wangjunxiang87928@126.com

YU Shihao was born in 1993. He received his B.S. degree in School of Electronic Information and Engineering from Beihang University, Beijing, China. He is currently studying in Beihang University for his master's degree. His current interests include radar target recognition in half space and artificial intelligence.
E-mail: shyu_ee@163.com

XIE Yongjun was born in 1968. He received his B.S., M.S., and Ph.D. degrees from Xidian University, Xi'an, China, in 1990, 1993, and 1996, respectively, in electronic engineering. From 1998 to 1999, he was with the University of Texas at Dallas, Dallas, TX, USA, as a post-doctoral research associate. From 1999 to 2001, he was with Duke University, Durham, NC, USA, as a post-doctoral research associate. In 2004, he was supported by the Program for the New Century Excellent Talents at the Ministry of Education, China. He is currently a professor in Beihang University. His research interests include electromagnetic theory, microwave technology, and mobile telecommunication.
E-mail: yjxie@buaa.edu.cn

ZHAO Yuxiong was born in 1998. He received his B.E. degree in software engineering from Beihang University. Currently, he is working toward his M.S. degree in data science and machine learning from National University of Singapore. His research interests include machine learning, computer vision and data mining.
E-mail: zhaoyuxiong@buaa.edu.cn